Rapid Communications

$^{40}Ca^{+}$ ion optical clock with micromotion-induced shifts below 1×10^{-18}

Y. Huang,[1,2] H. Guan,[1,2,*] M. Zeng,[1,2] L. Tang,[1,2] and K. Gao[1,2,3,†]

[1]*State Key Laboratory of Magnetic Resonance and Atomic and Molecular Physics, Wuhan Institute of Physics and Mathematics, Chinese Academy of Sciences, Wuhan 430071, China*

[2]*Key Laboratory of Atomic Frequency Standards, Wuhan Institute of Physics and Mathematics, Chinese Academy of Sciences, Wuhan 430071, China*

[3]*Center for Cold Atom Physics, Chinese Academy of Sciences, Wuhan 430071, China*

(Received 9 March 2018; published 22 January 2019)

We recently reported a $^{40}Ca^{+}$ optical clock comparison with an uncertainty at 5.5×10^{-17}, mainly limited by the excess micromotion shift. Here we report the progress made to reduce this shift and its uncertainty below 1×10^{-18} by precise measurement of the "*magic*" rf drive frequency Ω_0 at which the micromotion-induced scalar Stark shift and second-order Doppler shift cancel each other. Ω_0 is measured as $2\pi \times 24.801(2)$ MHz, and the differential static scalar polarizability $\Delta\alpha_0$ of the $^{40}Ca^{+}$ ion clock transition is measured as $-7.2677(21) \times 10^{-40}$ J m^2 V^{-2}. The blackbody radiation shift is then calculated to be 0.37913(12) Hz at 300 K considering the dynamic correction. The contribution of the blackbody shift coefficient to the uncertainty of the optical clock at room temperature has been reduced to the 3×10^{-19} level. With further improvements made to reduce the servo error, the total clock uncertainty is reduced to 2.2×10^{-17}, limited by the blackbody radiation field evaluation.

DOI: 10.1103/PhysRevA.99.011401

Optical clocks have made great advances in the past two decades [1–9] with uncertainties one to two orders of magnitude better than state-of-art Cs primary frequency standards [10,11]. The optical clocks with the lowest fractional frequency uncertainties reported to date are the $^{171}Yb^{+}$ ion clock [6] and the ^{87}Yb optical lattice clock [9], both having reached an uncertainty at the low 10^{-18} level. The performance of optical clocks promises a large variety of benefits [12], and scientists are working towards a redefinition of the *Système International* time unit using optical clocks [13,14].

In ion clocks, a potentially very significant source of frequency shift and uncertainty is the micromotion, which results from the interaction of the ion with the trapping rf electric fields. Micromotion occurs when the ion is not located at the nodal position of the trap's ac electric field. It has a few causes: Ion displacement caused by stray electric fields, ion thermal motion, and a phase difference between the trap electrodes. Methods to reduce the micromotion-induced shifts play an important role in the development of ion-based optical clocks. Generally an additional electric field is introduced to compensate the stray fields and reduce the excess micromotion [15]. The micromotion levels can be measured using various methods, for example, the rf-photon correlation technique and the sideband intensities measurement method [5,16]. In linear traps [2] and endcap traps [4–6], trimming of the wire lengths is used to keep the symmetry of the trap, reducing the micromotion due to a phase difference between the rf electrodes. The intrinsic micromotion contribution from the periodic displacement due to the secular motion can be greatly reduced by ground-state cooling the ion in three dimensions [17].

With the above methods, the micromotion-induced uncertainty can be reduced to below 1×10^{-17}. The ion-based optical clocks with the lowest uncertainty to date, the $^{27}Al^{+}$ [2] and $^{171}Yb^{+}$ [6] clocks, are both still limited by the micromotion effect. We recently reported a 5.5×10^{-17} level frequency comparison of two $^{40}Ca^{+}$ optical clocks, also limited by the excess micromotion shift [18,19].

In this Rapid Communication, we report the progress made to reduce the micromotion-induced shift below 1×10^{-18} by precisely determining the "*magic*" rf drive frequency Ω_0 [4] of the $4s\,^2S_{1/2} - 3d\,^2D_{5/2}$ clock transition of $^{40}Ca^{+}$. The measurement is performed by comparing two $^{40}Ca^{+}$ ion clocks using one of them as a reference whereas the other is operated with intentionally large micromotion levels to make an accurate measurement.

An additional test was performed to validate the expected large suppression of the micromotion shifts at the magic drive frequency. For this test, both clocks, Clock1 and Clock2, were operated at the magic drive frequency, and their frequencies were compared under two extreme conditions. In one comparison experiment, the micromotion was minimized as well as permitted by the apparatus. In a second comparison experiment, the micromotion of Clock2 was increased to high levels. No change in frequency was observed at the 10^{-16} level, indicating that the residual micromotion shifts are below 1×10^{-18} when the micromotion is minimized.

The differential static scalar polarizability $\Delta\alpha_0$ is a key parameter in the evaluation of the blackbody radiation (BBR) shift, another important source of uncertainty in optical clocks. $\Delta\alpha_0$ is determined from the magic drive frequency Ω_0 with an uncertainty of 0.03%, which is ~40 times better than

*guanhua@wipm.ac.cn
†klgao@wipm.ac.cn

the $\sim 1.15\%$ uncertainty of the best atomic structure calculations for the S-D transition of $^{40}Ca^{+}$ [20]. This measurement of $\Delta\alpha_0$ has the lowest fractional uncertainty of the currently studied ion-based optical clocks. With state preparation [21] and an additional integration servo introduced in the lock to the clock transition Zeeman components, the clock stability was improved, and the servo error was reduced to the 10^{-18} level. With the above improvements, the total clock uncertainty is reduced to 2.2×10^{-17}, limited by the BBR field evaluation like most state-of-art ion or neutral atom optical clocks [4–7].

In a Paul trap, the overall micromotion-induced scalar Stark shift and second-order Doppler shift $\Delta\nu_\mu$ can be calculated as [4,15]

$$\frac{\Delta\nu_\mu}{\nu_0} \simeq -\frac{1}{2}\left[\left(\frac{e}{m\Omega c}\right)^2 + \frac{\Delta\alpha_0}{h\nu_0}\right]\langle \boldsymbol{E}^2\rangle, \tag{1}$$

where e is the elementary charge, m is the ion mass, Ω is the trap drive angular frequency, c is the speed of light, and ν_0 is the clock transition frequency of ~ 411 THz. $\Delta\alpha_0 = \alpha_0(e) - \alpha_0(g)$ is the differential static scalar polarizability of the clock transition where e and g refer to the excited and ground states, respectively. In the first-order approximation, if the ion trap is operated with a drive frequency of $\Omega_0 \simeq \frac{e}{mc}\sqrt{-\frac{h\nu_0}{\Delta\alpha_0}}$, the micromotion-induced scalar Stark shift and second-order Doppler shift would cancel each other, and then the total micromotion-related shift vanishes. This is only possible for transitions with negative differential polarizability. The frequency Ω_0 is so-called the *magic* trap drive frequency [4].

For the measurement of Ω_0, the rf driving source of the two clocks was redesigned such that the drive frequency could be continuously tuned from 22 to 27 MHz while keeping the ion trapped. A narrow-band tunable frequency filter was added to the rf drive to suppress the higher-order harmonic components of the rf driving source. The endcap and compensation electrodes were also better low-pass filtered. With these improvements, the heating rate of the trap was reduced by half to ~ 0.01 mK/ms or ~ 250 quanta/s for our measured averaged secular frequency of $\sim 2\pi \times 1.7$ MHz. To begin with, the rf drive frequencies of both clocks were tuned to 24.8500(1) MHz, close to the *magic* drive frequency of 24.7(3) MHz derived from the calculation of $\Delta\alpha_0$ by Safronova and Safronova [20]. The micromotions of both clocks were minimized after which both clocks were reevaluated with uncertainties of $\sim 3 \times 10^{-17}$, limited by the evaluation of the BBR shift. The frequency comparison between two clocks was made, showing agreement at the evaluated uncertainty. The rf drive frequency of Clock1 was kept constant during the whole experiment. A dc offset voltage was added to the vertical compensation electrode of Clock2 to produce relatively large micromotion levels. The displaced ion was driven by the local pseudopotential electric-field amplitude estimated at ~ 3300 V/m in the vertical direction [15]. The micromotion was still minimized in the horizontal direction, which prevented Doppler broadening of the cooling and clock transitions for the horizontally aligned laser beams. Thus the probe laser could be easily locked to the Zeeman components of the clock transition despite the relatively large transverse micromotion amplitude.

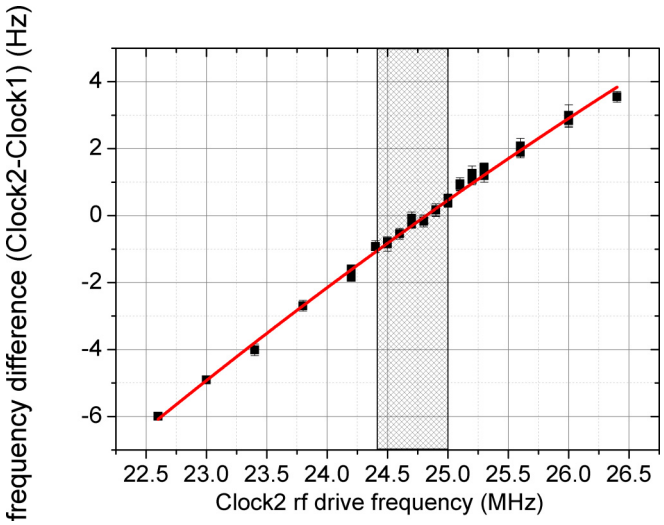

FIG. 1. Frequency difference between the two $^{40}Ca^{+}$ ion clocks as a function of the rf drive frequency of Clock2 operated with intentionally high micromotion levels. The curve is a fit to the data using a polynomial to determine Ω_0. The fit gives $\Omega_0 = 2\pi \times 24.81(1)$ MHz. The slope at $f = \Omega_0/2\pi$ can be used to determine the mean-squared electric-field $\langle \boldsymbol{E}^2\rangle$ [4]. The shaded area illustrates the uncertainty of a theoretical result [20].

Details of the clock comparison experimental setup can be found in our previous work [18]. Briefly speaking, two ions are separately trapped with miniature Paul traps [22], the ambient magnetic field is reduced by two layers of magnetic shielding, and then a background magnetic field of $\sim 0.5\ \mu$T is applied to split the Zeeman components. Each clock laser beam passes through an acousto-optic modulator to match the clock transition. The clock laser synchronously probes the two ions. Taking Clock1 as a frequency reference, the micromotion shifts of Clock2 can be measured in frequency comparisons. The rf drive frequency of Clock2 is scanned for the study of the magic drive frequency. Clock comparisons of ~ 4 h are made at each trap drive frequency, giving a frequency shift measurement uncertainty of ~ 50 mHz ($\sim 1 \times 10^{-16}$). Before each measurement, all of the systematic shifts except for the micromotion effect are evaluated for Clock2 to make sure the measured frequency difference of the two clocks is primarily caused by the micromotion effect. The trap voltage amplitude was adjusted to keep the ion secular frequencies constant with different rf driving frequencies [4]. The trap voltage amplitude itself proved to be rather stable during the 4-h experiments; the secular frequencies were measured by probing the clock transition carrier and secular motion sidebands every 10 min, showing that the fluctuations in secular frequencies were within 3 kHz during the 4-h experiments.

Figure 1 shows the frequency difference of the two clocks as a function of the rf driving frequency of Clock2. The data were taken within an ~ 2-week period in a random order. The whole data set was taken with the same ions loaded. The stray electric field was measured to be almost constant during the experiments. The uncertainty of each data point in Fig. 1 has two components: One is the statistical uncertainty given by the clock comparison data; the other is the uncertainty in setting

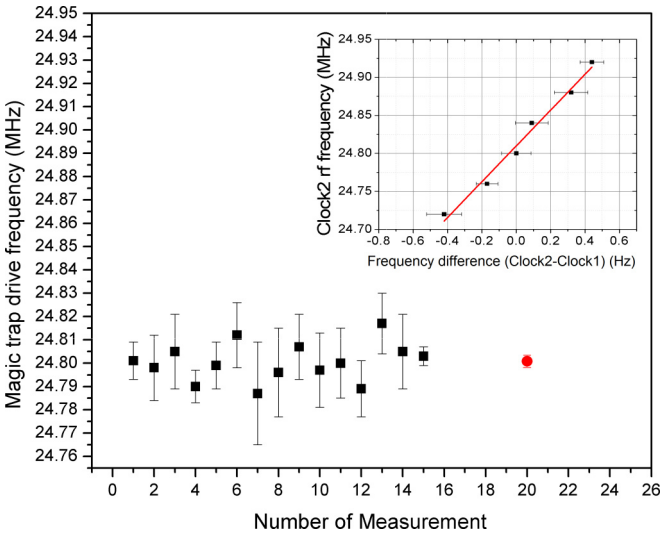

FIG. 2. Measurement of Ω_0 obtained by scanning the rf drive frequency of Clock2 from 24.7 to 24.95 MHz. Fifteen scans were recorded (data shown as black squares). The corresponding weighted mean of Ω_0 is shown by the red circle. The inset shows the data taken in one of the scans and a linear fit through the data. The linear fit is used to determine Ω_0, the drive frequency at which the two ion clocks have the same optical frequency.

the trap voltage. Variations in trap voltage change the micromotion amplitude, thus, causing an additional uncertainty in the frequency difference between the two clocks.

To reduce the measurement statistical uncertainty of Ω_0, the drive frequency of Clock2 was repeatedly and randomly scanned from 24.7 to 24.95 MHz. Linear fits were taken to obtain Ω_0 after each scan. Figure 2 shows the measurement of Ω_0 obtained with 15 such scans. The inset shows the data taken in one of the scans and their linear fits. The corresponding weighted mean gives $\Omega_0 = 2\pi \times 24.801(2)$ MHz. To make an accurate measurement of Ω_0, the frequency offset between the two clocks has been evaluated. The dominant uncertainty is from the BBR shift. The frequency offset between the two clocks is evaluated as $-7(11)$ mHz. Each data point in Figs. 1 and 2 was corrected for the evaluated frequency offset during its measurement.

Setting the trap drive frequency close to the precisely measured Ω_0, $2\pi \times 24.8$ MHz in our case, suppresses significantly the net micromotion-induced frequency shift and uncertainty. The $\langle \boldsymbol{E}^2 \rangle$ from micromotion was minimized and evaluated with a method that we previously used in Ref. [18]. This method is based on measurements of the micromotion sideband and carrier intensity ratio and on the ion displacement observed in the electron-multiplying CCD camera.

The value of $\langle \boldsymbol{E}^2 \rangle$ is estimated to be $< (200\ \mathrm{V/m})^2$, which corresponds to a total excess micromotion-induced shift of $< 1 \times 10^{-18}$ at the trap drive frequency of 24.8 MHz, determined by the measured differential polarizability.

Additional clock comparison experiments were performed to further prove that the micromotion-induced shift is really suppressed below a fractional uncertainty of 1×10^{-18}. Clock frequency differences were measured to be $< 1 \times 10^{-16}$ when running Clock2 both with strong micromotion levels $\sim (3300\ \mathrm{V/m})^2$ and with weak micromotion levels $(200\ \mathrm{V/m})^2$. $\langle \boldsymbol{E}^2 \rangle$ is evaluated by measuring the slope as mentioned in Fig. 1 in the stronger micromotion case and evaluated with the method in Ref. [18] in the weaker micromotion case. Since the micromotion of Clock1 is kept minimized during the experiments, the measurements show that increasing the Clock2 micromotion by $> 270\times$ only increases the shift to $< 1 \times 10^{-16}$, which means that the micromotion induced shift in Clock2 is reduced to a level of $< 4 \times 10^{-19}$ when $\langle \boldsymbol{E}^2 \rangle$ is minimized to $< (200\ \mathrm{V/m})^2$.

State-of-art theoretical calculations of $\Delta\alpha_0$ have uncertainties at the 1% level [20,23–25], which contribute uncertainties at the 10^{-17} level for the clock transition frequencies. Compared to theory, $\Delta\alpha_0$ can be measured experimentally with an uncertainty of one to three orders of magnitude smaller. In neutral atom optical clocks, such as Yb [26] and Sr [27], $\Delta\alpha_0$ is obtained by measuring the dc Stark shift caused by applied dc electric fields. For ion-based optical clocks, $\Delta\alpha_0$ for the octupole transition in Yb^+ was obtained by measuring clock shifts under near-infrared laser radiation with different wavelengths [6]; $\Delta\alpha_0$ of Sr^+ was obtained by measuring the trap drive frequency at which the micromotion shift comes to 0 [4].

To determine $\Delta\alpha_0$ from Ω_0 with a higher accuracy, the ion motion in Clock2 has to be studied in more detail. In our case, micromotion at the trap drive frequency Ω_0 is by far the dominant component, yet there is still motion at higher-order harmonics $n\Omega_0$ and thermal motion sidebands at the radial and axial secular frequencies [4]. Based on the calculation made by Dubé *et al.* in Sr^+ clocks [4], we find that, in our case, only the motion with frequencies at Ω_0 and $2\Omega_0$ caused by ion displacement should be considered. The thermal motion sidebands and motion at the other harmonics $n\Omega_0$ will only cause frequency shifts at the millihertz level or even less, which is negligible in our measurement compared to the evaluated comparison uncertainty of 11 mHz.

A general expression for the total micromotion shift over the trap drive harmonics of motion is given by [4]

$$\Delta\nu_\mu = \frac{\nu_0}{2} \sum_i \sum_{n=1}^{\infty} \left[\frac{\Delta\alpha_0}{h\nu_0} + \frac{1}{n^2} \left(\frac{e}{m\Omega_0 c} \right)^2 \right] \times \langle \boldsymbol{E}_i^2(n\Omega) \rangle, \qquad i = r, z, \tag{2}$$

where i is a summation index over the radial "r" and axial "z" directions in the trap, $\langle \boldsymbol{E}_i^2(n\Omega) \rangle$ is the mean-squared electric field at the frequency $n\Omega$.

By only taking into account terms with frequencies Ω and 2Ω, one can solve Eq. (2) to obtain [4]

$$\Delta\alpha_0 \simeq -\frac{h\nu_0}{\Omega_0^2} \left(\frac{e}{mc} \right)^2 \left[\frac{(1+\rho_z/4) + \xi(1+\rho_r/4)}{(1+\rho_z) + \xi(1+\rho_r)} \right], \tag{3}$$

where $\xi \equiv \langle \boldsymbol{E}_r^2(\Omega) \rangle / \langle \boldsymbol{E}_z^2(\Omega) \rangle$, $\rho_i \equiv \langle \boldsymbol{E}_i^2(2\Omega) \rangle / \langle \boldsymbol{E}_i^2(\Omega) \rangle$, $\imath = r, z$, and ρ_i can be obtained by measuring the trap Mathieu parameters a_i and q_i [28] as [4]

$$\rho_i = \left(\frac{4q_i}{a_i - 16} \right)^2, \qquad i = r, z. \tag{4}$$

The Mathieu parameters a_i and q_i can be calculated from the measured radial and axial secular frequencies by solving the

equations [29,30],

$$\left(\frac{2\omega_i}{\Omega_0}\right)^2 = a_i - \left(\frac{a_i - 1}{2(a_i-1)^2 - q_i^2}\right)q_i^2 - \left(\frac{5a_i + 7}{32(a_i-1)^3(a_i-4)}\right)q_i^4, \quad i = r, z \tag{5}$$

where ω_i, $i = r, z$ are the measured radial or axial secular frequencies ω_r or ω_z, respectively, with the trap drive frequency at Ω_0.

To sum up, for the precise measurement of $\Delta\alpha_0$, one needs to obtain ω_r, ω_z, and ξ beside the measured Ω_0. At $\Omega_0 = 2\pi \times 24.801(2)$ MHz, the secular frequencies are measured as $\omega_r = 2\pi \times 1.239(3)$, and $\omega_z = 2\pi \times 2.528(3)$ MHz. From which ρ_i, $i = r, z$ are calculated as $\rho_r = 0.001\,30(4)$, $\rho_z = 0.0052(1)$. The parameter ξ depends on the micromotion electric-field direction. If β defines the angle between the micromotion electric field and the trap z axis, we have $\tan^2\beta = \langle \boldsymbol{E}_r^2\rangle/\langle \boldsymbol{E}_z^2\rangle$, and then we have [4]

$$\xi = \left(\frac{1+\rho_z}{1+\rho_r}\right)\tan^2\beta. \tag{6}$$

In our case, the micromotion electric-field direction should be vertical since the ion has been displaced in the vertical direction. The very small micromotion sideband observed in the laser beam direction also shows that the micromotion direction is perpendicular to the laser beam direction. However, since the vertical compensation electrode is not exactly vertical, there is no other viewport access for micromotion sideband detection, and β cannot be precisely measured by observing the micromotion sidebands. Thus, the method used in Ref. [4] is adopted to determine β. The tensor Stark shift is measured with the magnetic field aligned with the trap axis z: From the slope with respect to m_J^2 of the tensor Stark shift $\Delta\nu_{\text{tensor}}$, one can obtain β by solving the equation [31],

$$\frac{\partial(\Delta\nu_{\text{tensor}})}{\partial m_J^2} = -\frac{3\alpha_2}{40h}(3\cos^2\beta - 1)\langle \boldsymbol{E}^2\rangle, \tag{7}$$

where α_2 is the $D_{5/2}$ state tensor polarizability, which has been theoretically calculated by Safronova and Safronova [20]. The variation with m_J^2 is obtained by locking the clock laser to three pairs of Zeeman components with different $D_{5/2}$ state magnetic sublevels m_J^2. $\langle \boldsymbol{E}^2\rangle$ can be obtained from the slope of the clock comparison data at Ω_0. Taking into account the alignment uncertainty of the magnetic field with the trap axis, the tensor Stark shift measurement gives $\beta = 85(5)^\circ$ and $\xi > 32$. This result is in agreement with our trap geometry because the trap axis is on the horizontal plane [18,19].

With the measured values of Ω_0, ρ_r, ρ_z, and ξ, $\Delta\alpha_0$ is then calculated as $-7.2677(21) \times 10^{-40}\,\text{J m}^2\,\text{V}^{-2}$ from Eq. (2).

Table I gives the uncertainty budget of $\Delta\alpha_0$. Calculation shows that the first-order approximation result from $\Delta\alpha_0 \simeq -\frac{h\nu_0}{\Omega_0^2}(\frac{e}{mc})^2$ only overestimates $\Delta\alpha_0$ by $\sim 0.1\%$ for our experimental conditions. The total uncertainty of our measurement is limited by the clock comparison uncertainty. The measurement of $\Delta\alpha_0$ reported here is in excellent agreement with the value of $-7.31(8) \times 10^{-40}\,\text{J m}^2\,\text{V}^{-2}$ obtained in recent theoretical calculations [20].

TABLE I. Uncertainty budget of the measurement of the differential scalar polarizability of the S-D transition of $^{40}Ca^+$.

Parameter	Value	$\Delta\alpha_0$ uncertainty ($10^{-43}\,\text{J m}^2\,\text{V}^{-2}$)
Ω_0	24.801(2) MHz	1.2
β	85(5)°	0.5
ρ_r	0.00130(4)	
ρ_z	0.0052(1)	0.7[a]
Evaluated clock		
Frequency offset	−7(11) mHz[b]	1.5
Total		2.1

[a]Uncertainty due to ρ_r and ρ_z.
[b]$\Delta\nu$(Clock2) − $\Delta\nu$(Clock1).

The BBR shift uncertainty is also greatly reduced by measuring the magic rf drive frequency. The BBR shift for the state i can be calculated as [32]

$$\Delta\nu_{\text{BBR},i} = -\frac{1}{2h}(831.943\ \text{V/m})^2\left(\frac{T}{300K}\right)^4 \times \alpha_{0,i}(1+\eta_i), \qquad i = e, g, \tag{8}$$

where h is Planck's constant, T is the BBR field temperature, and e and g refer to the excited and ground states, respectively. η_i is a small correction parameter accounting for the dynamic aspect of the BBR field.

It can be inferred from Eq. (8) that the BBR shift can be precisely evaluated only if the BBR field temperature T, the differential static scalar polarizability $\Delta\alpha_0$, and the dynamic correction η_i are all calculated or measured with high precision. For most optical clocks, η_i is small and contributes an uncertainty at the 10^{-18} level or less [4,6,7,20,26]. The BBR field temperature T can be evaluated by measuring with calibrated temperature sensors with consideration for the temperature nonuniformity in the case of ion clocks due to the rf currents flowing in the trap electrodes. The BBR field temperature can be evaluated with an uncertainty at the kelvin level by this method. With better modeling and new trap designs that have better temperature uniformity, it is possible to evaluate the BBR field temperature with subkelvin uncertainty, corresponding to a clock transition uncertainty at the 10^{-18} level.

To calculate the BBR shift, the dynamic correction η has to be evaluated. The dynamic fractional correction to the total BBR shift can be approximated by

$$\eta = \frac{80\pi^2}{63(2J_g+1)k_BT\alpha_g(0)}\sum_n \frac{|\langle g\|D\|n\rangle|^2}{y_n^3} \times \left[1 + \frac{21\pi^2}{5y_n^2} + \frac{336\pi^4}{11y_n^4}\right]. \tag{9}$$

Here D is the dipole transition operator, and $y_n = \omega_{ng}/T$. Correspondingly, the dynamic correction to the BBR shift of the Ca^+ clock transition frequency is

$$\Delta\nu^{\text{dyn}}_{3D_{5/2}\to 4S_{1/2}} = -\tfrac{2}{15}(\alpha\pi)^3(k_BT)^4 \times [\alpha_{3D_{5/2}}(0)\eta_{3D_{5/2}} - \alpha_{4S_{1/2}}(0)\eta_{4S_{1/2}}]/h, \tag{10}$$

and the systematic uncertainty caused by $\Delta\eta$ is evaluated by

$$\frac{2(\alpha\pi)^3(k_BT)^4}{15h\nu}\sqrt{[\Delta\eta_{3D_{5/2}}\alpha_{3D_{5/2}}(0)]^2+[\Delta\eta_{4S_{1/2}}\alpha_{4S_{1/2}}(0)]^2} \simeq 1.1\times10^{-19}. \quad (11)$$

Using the relativistic configuration interaction plus core polarization method [33], we obtain $\eta = 0.001\,22(4)$ and $\alpha_0 = 1.244(12)\times10^{-39}\ \mathrm{J\,m^2\,V^{-2}}$ or 75.46(72) a.u. for the $4S_{1/2}$ state, which agrees well with the value of 76.1(5) a.u. in Ref. [20], and $\eta = 0.004\,37(13)$ with $\alpha_0 = 5.408(40)\times10^{-39}\ \mathrm{J^{-1}\,m^{-2}\,V^2}$ or 32.80(24) a.u. for the $3D_{5/2}$ state. So the dynamic correction to the Ca^+ BBR shift is $\Delta\nu^{\mathrm{dyn}}_{3D_{5/2}\to4S_{1/2}} = -0.441$ mHz, and the systematic uncertainty caused by the dynamic correction is evaluated as 1.1×10^{-19}. Together with our measured value of $\Delta\alpha_0$, from Eq. (8) the BBR shift is calculated as 0.379 13(12) Hz at 300 K. The contribution of the BBR coefficient to the $^{40}Ca^+$ ion clock uncertainty has been reduced from 1.1×10^{-17} to 3×10^{-19}. With suppression of the BBR field temperature uncertainty to the subkelvin level at room temperature, the total BBR shift uncertainty reaches the 10^{-18} level. For example, a BBR temperature uncertainty of 0.1 K would give an uncertainty of 1.3×10^{-18}.

The clock uncertainty caused by the servo error was also reduced. In our experiments, the locking software is always tracking the Zeeman transitions with the probe laser, which is drifting. The probe laser has a nonlinear drift that cannot be easily compensated. This drift can cause a servo tracking shift and error, which can be inferred from the small residual errors in the quantum jump imbalances recoded by the software. In our case, the servo error is reduced by introducing the state preparation technique [34] before the clock interrogations. The observed clock transition is narrowed to ~4 Hz with improvements made to the clock lasers [35] and reduction of the air turbulence. Narrower linewidths help improve the clock stability by reducing the servo tracking errors. An additional integration servo loop was also added to make the servo error even smaller. With these improvements, the servo error is evaluated as $2(8)\times10^{-18}$, ~2.5 times smaller than in our previous evaluation [18].

Table II summarizes the systematic evaluation result. With the improvements reported here, the total uncertainty for the $^{40}Ca^+$ optical clock is reduced to 2.2×10^{-17}, limited by the BBR field evaluation, such as most state-of-art ion or neutral atom optical clocks [4–7]. This Rapid Communication provides significant improvements showing that the $^{40}Ca^+$ ion clock uncertainties caused by both the BBR shift coefficient and the excess micromotion have been reduced to the 10^{-19} level. With a suppression of the BBR field temperature uncertainty to the subkelvin level at room temperature in the future, the BBR shift uncertainty and the total clock uncertainty can be reduced to the 10^{-18} level.

To summarize, by setting the trap drive frequency to the precisely measured magic trap drive frequency, the micromotion-induced shift, previously limiting our clock comparison uncertainty, is reduced to below 1×10^{-18} according to the evaluation result. The differential static scalar polarizability $\Delta\alpha_0$ of the $4s\,^2S_{1/2} - 3d\,^2D_{5/2}$ transition of $^{40}Ca^+$ is also measured with an uncertainty ~40× smaller than the previous best determination obtained by theoretical calculation. With our precisely measured value of $\Delta\alpha_0$ and calculated dynamic correction, the clock uncertainty due to the knowledge of the BBR shift coefficient was determined as 0.12 mHz at 300 K, giving a contribution of 3×10^{-19} to the clock uncertainty. The clock stability was improved, and the servo error was reduced to the 10^{-18} level. With the above-mentioned improvements, the overall $^{40}Ca^+$ optical clock uncertainty was reduced to 2.2×10^{-17} and is mainly limited by the BBR field evaluation uncertainty of 1.6 K. A further study on the evaluation of the BBR field is required, and we are planning to house the ion trap in a liquid-nitrogen temperature environment to obtain further reductions of the BBR shift uncertainty. With reductions of the shifts and their uncertainties mentioned above, a $^{40}Ca^+$ ion clock with an uncertainty at the 10^{-18} level can be achieved.

TABLE II. Systematic shifts and uncertainties for the evaluation of the $^{40}Ca^+$ optical clock. Some systematic contributions with shift and uncertainties $< 1\times10^{-19}$ are negligible and therefore not shown in the table.

Effect	Shift (10^{-18})	Uncertainty (10^{-18})
BBR field evaluation (temperature)	863	19
BBR coefficient $\Delta\alpha_0$ including dynamic correction	0	0.3
Excess micromotion	0	0.4
Second-order Doppler (thermal motion)	−11.4	5.5
ac Stark shift	1.2	1.3
Residual quadrupole	0	3.6
Zeeman effect	0	1.5
Servo	2.2	7.6
Total	855	22

We thank P. Dubé for his help and fruitful discussions on the measurement of the differential polarizability, J. Ye for the suggestion on the micromotion shift measurement, D. Leibrandt, and N. Huntemann for the discussion on the method of reducing the servo uncertainty. We thank W. Bian for the early work. This Rapid Communication was supported by the National Key R&D Program of China (Grants No. 2017YFA0304401, No. 2018YFA0307500, and No. 2017YFA0304404), the Natural Science Foundation of China (Grants No. 91736310, No. 11774388, No. 11634013, and No. 11622434), the Strategic Priority Research Program of the Chinese Academy of Sciences (Grant No. XDB21030100), CAS Youth Innovation Promotion Association (Grants No. 2015274 and No. 2018364), and Hubei Province Science Fund for Distinguished Young Scholars (Grant No. 2017CFA040).

[1] S. L. Compbell, R. B. Hutson, G. E. Marti *et al.*, Science **358**, 90 (2017).

[2] C. W. Chou, D. B. Hume, J. C. J. Koelemeij, D. J. Wineland, and T. Rosenband, Phys. Rev. Lett. **104**, 070802 (2010).

[3] T. Rosenband, D. B. Hume, P. O. Schmidt *et al.*, Science **319**, 1808 (2008).

[4] P. Dubé, A. A. Madej, M. Tibbo, and J. E. Bernard, Phys. Rev. Lett. **112**, 173002 (2014).

[5] G. P. Barwood, G. Huang, H. A. Klein *et al.*, Phys. Rev. A **89**, 050501 (2014).

[6] N. Huntemann, C. Sanner, B. Lipphardt, C. Tamm, and E. Peik, Phys. Rev. Lett. **116**, 063001 (2016).

[7] T. L. Nicholson, S. L. Campbell, R. B. Hutson *et al.*, Nat. Commun. **6**, 6896 (2015).

[8] I. Ushijima, M. Takamoto, M. Das *et al.*, Nat. Photon. **9**, 185 (2015).

[9] W. F. McGrew, X. Zhang, R. J. Fasano *et al.*, Nature (London) **564**, 87 (2018).

[10] R. Li, K. Gibble, and K. Szymaniec, Metrologia **48**, 283 (2011).

[11] S. Weyers, V. Gerginov, M. Kazda *et al.*, Metrologia **55**, 789 (2018).

[12] A. D. Ludlow, M. M. Boyd, J. Ye *et al.*, Rev. Mod. Phys. **87**, 637 (2015).

[13] P. Gill, Philos. Trans. R. Soc. A **369**, 4109 (2011).

[14] F. Riehle, C. R. Phys. **16**, 506 (2015).

[15] D. J. Berkeland, J. D. Miller, J. C. Bergquist *et al.*, J. Appl. Phys. **83**, 5025 (1998).

[16] J. Keller, H. L. Partnera, T. Burgermeister, and T. E. Mehlstäubler, J. Appl. Phys. **118**, 104501 (2015).

[17] J. S. Chen, S. M. Brewer, D. B. Hume *et al.*, Phys. Rev. Lett. **118**, 053002 (2017).

[18] Y. Huang, H. Guan, P. Liu *et al.*, Phys. Rev. Lett. **116**, 013001 (2016).

[19] Y. Huang, H. Guan, P. Liu *et al.*, Appl. Phys. B. **123**, 166 (2017).

[20] M. S. Safronova and U. I. Safronova, Phys. Rev. A **83**, 012503 (2011).

[21] M.-Y. Zeng, Y. Huang, H. Shao *et al.*, Chin. Phys. Lett. **35**, 074202 (2018).

[22] Y. Huang, Q. Liu, J. Cao *et al.*, Phys. Rev. A **84**, 053841 (2011).

[23] D. Jiang, B. Arora, M. S. Safronova *et al.*, J. Phys. B: At. Mol. Opt. Phys. **42**, 154020 (2009).

[24] S. G. Porsev, A. D. Ludlow, M. M. Boyd, and J. Ye, Phys. Rev. A **78**, 032508 (2008).

[25] V. A. Dzuba and A. Derevianko, J. Phys. B: At. Mol. Opt. Phys. **43**, 074011 (2010).

[26] J. A. Sherman, N. D. Lemke, N. Hinkley *et al.*, Phys. Rev. Lett. **108**, 153002 (2012).

[27] T. Middelmann, S. Falke, C. Lisdat, and U. Sterr, Phys. Rev. Lett. **109**, 263004 (2012).

[28] D. J. Wineland, W. M. Itano, and R. S. Van Dyck, Jr., in *High-Resolution Spectroscopy of Stored Ions*, edited by D. Bates and B. Bederson, Advances in Atomic and Molecular Physics Vol. 19 (Academic, New York, 1983), pp. 135–186.

[29] P. J. Blythe, S. A. Webster, K. Hosaka1, and P. Gill, J. Phys. B: At. Mol. Opt. Phys. **36**, 981 (2003).

[30] G. P. Barwood, H. S. Margolis, G. Huang, P. Gill, and H. A. Klein, Phys. Rev. Lett. **93**, 133001 (2004).

[31] P. Dubé, A. A. Madej, Z. Zhou, and J. E. Bernard, Phys. Rev. A **87**, 023806 (2013).

[32] S. G. Porsev and A. Derevianko, Phys. Rev. A **74**, 020502 (2006).

[33] J. Jiang, L. Jiang, X. Wang *et al.*, Phys. Rev. A **96**, 042503 (2017).

[34] P. Dubé, A. A. Madej, A. Shiner, and B. Jian, Phys. Rev. A **92**, 042119 (2015).

[35] W. Bian, Y. Huang, H. Guan *et al.*, Rev. Sci. Instrum. **87**, 063121 (2016).